Wideband Analysis of Periodic Structures at Oblique Incidence by Material Independent FDTD Algorithm

Bin Liang, Ming Bai, Hui Ma, Naiming Ou, and Jungang Miao

***Abstract*—A novel implementation of the finite difference time domain (FDTD) algorithm to analyze periodic structures over a wideband with oblique incident waves is presented. Based on the field transformation treatment, the method splits each component of the transformed fields of the electric displacement vector and the magnetic induction intensity vector into three parts in a simple manner. This treatment is independent of material and easily implemented, so that it could be utilized in a wide range of periodic structure analysis. The advantage of the method is demonstrated through two numerical examples. One is Jerusalem cross frequency selective surfaces (JCFSS) with anisotropic lossy media in the millimeter wave band, and excited by the TM wave at $\theta = 20^\circ$ and the TE wave at $\theta = 45^\circ$, respectively. Another is a photonic periodic structure with rectangular holes for the visible and infrared bands, where it acts as a dispersive medium, with the incident TE plane wave at $\theta = 30^\circ$. The results are in good agreement with those of CST Microwave Studio, and thereby the validity of the method is verified.**

***Index Terms*—Finite difference time domain (FDTD), material independent, oblique incidence, periodic structures, wideband.**

I. Introduction

With the increasing development and use of periodic structures in electromagnetic applications, such as frequency selective surfaces (FSS) [1]–[3], electromagnetic band gap (EBG) devices, phased antenna arrays and random rough surfaces, the analysis of periodic structures is extensively required. Since the periodic structures can be considered infinite in 2-D horizontal directions in many cases, only an individual unit cell need be analyzed instead of the entire structures, according to the Floquet theory [4]. Such treatment brings significant saving in memory usage and computation time, and has been widely utilized in many numerical methods.

As a well-developed technique, the finite difference time domain (FDTD) algorithm has been widely adopted in the analysis of periodic structures, owing to its wideband capability of calculation and the advantage of versatile modeling [5]. For a normal incident plane wave, a wideband response can be simply obtained by utilizing the periodicity of a unit cell because there is no phase shift between the two corresponding boundaries. However, when the plane wave is obliquely incident, an obstacle caused by the phase shift in the frequency domain and corresponding time delay in the time domain is encountered. To overcome this, Harms proposed the dual plane wave method [6] in 1994, but each calculation is only fixed on one single frequency. To realize wideband calculations, the split-FDTD method [7] was proposed in 1998, which introduces a set of auxiliary variables to remove the time delay. Further to overcome the restraint of the Courant stability criterion of split-FDTD technique which is introduced by the extra time terms, some unconditionally stable methods for 2-D periodic structures [8]–[10] and weakly conditionally stable methods for 3-D structures [11] have been proposed in recent years. It is noticed that all these techniques are based on the implicit relations between electric fields and magnetic fields, or their transformation without the time gradient terms. They substitute one or more sets of Maxwell's equations into another, and finally obtain one equation containing only one field component. By solving a perturbed tri-diagonal system [11], such a component can be calculated efficiently and the other field components can be obtained by substituting into other equations.

It is worthwhile to point out that although these developments have brought the advantage of unconditional or weakly conditional stability, the inherent coupling of electric and magnetic fields and the necessity of equation substitution result in a limitation caused by the dependence on the type of material. All the materials considered and implemented in [7]–[11] are simple media, since the derivation process and the resulting formulas for complicated media will be diverse and much more complicated, such as for anisotropic, lossy and dispersive mediums.

In this paper, a simple treatment based on the field transformation method (FTM) by removing the time gradient term is proposed. As an effective treatment to remove the time delay on corresponding boundaries, the FTM has been utilized in all of the techniques dealing with wideband FDTD analysis of periodic structures at oblique incidence [7]–[11]. Meanwhile, the auxiliary differential equation (ADE) treatment was proposed for implementing perfectly matched layers (PML) and truncating general mediums [12]. This has been widely used, owing to its material independence and uniformity of the formula between the calculation domain and PML. Similar to the ADE treatment, this method splits each transformed component of the electric displacement vector and the magnetic induction intensity vector into two terms, but additionally introduces another term with respect to the time derivative. Therefore, this method retains both the wideband capability of FDTD and the advantage of material independence offered by ADE treatment. Although the method requires increasingly small time steps with the increase of incident angle and even infinitely small

Manuscript received November 14, 2012; revised February 18, 2013; accepted October 09, 2013. Date of publication November 01, 2013; date of current version December 31, 2013. This work was supported by the National Basic Research Program of China (973 Program) under Grant 2012CB315601.

The authors are with the Microwave Engineering Laboratory, Beihang University, Beijing 100191, China (e-mail: mbai@buaa.edu.cn).

Color versions of one or more of the figures in this paper are available online at http://ieeexplore.ieee.org.

Digital Object Identifier 10.1109/TAP.2013.2287896

time step at grazing incidence, it has two advantages. First, the resulting formulas are clear and straightforward, becoming uniform in both the calculation domain and PML region. Second and most significant, the method is independent of material, so that it could be used for solving periodic structures with any type of media when the incident angle is not close to 90°. Only transforming the equations of the constitutive relations like at normal incidence is required.

This paper is organized as follows. In Section II, the novel method of splitting the transformed fields of the electric displacement vector and the magnetic induction intensity vector is proposed and implemented, with the detailed derivation of the resulting formulations presented. Additionally to clarify the stability condition and the approach of adding an oblique incident wave as the exciting source, some further discussions are provided. In Section III, two numerical examples with different materials in different bands and applications are given; the results are compared with those by commercial CST software. Finally, this paper is concluded in Section IV.

II. Mathematical Formulation

A. Formulation for Updating the Fields

Using the stretched coordinate formulation [12], [13], the frequency domain modified Maxwell's equations can be written as

$$\nabla_s \times \mathbf{H} = j\omega\mathbf{D} \tag{1}$$

$$\nabla_s \times \mathbf{E} = j\omega\mathbf{B} \tag{2}$$

where ∇_s is

$$\nabla_s = \hat{i}_x S_x^{-1}\partial x + \hat{i}_y S_y^{-1}\partial y + \hat{i}_z S_z^{-1}\partial z \tag{3}$$

where $\partial x, \partial y$ and ∂z are the space derivatives with respect to x, y and z, and $S_\eta(\eta = x, y, z)$ are the stretched coordinate variables, which are obtained as

$$S_\eta = 1 + \sigma_\eta / j\omega\varepsilon_0 \quad (\eta = x, y, z) \tag{4}$$

where σ_η is the conductivity profile along the η-direction in the PML region [12] and is zero in the calculation region.

In (1) and (2), $\mathbf{E}$ and $\mathbf{H}$ are the electric and magnetic field vectors respectively, and $\mathbf{D}$ and $\mathbf{B}$ are the electric displacement vector and the magnetic induction intensity vector. Their relations can be written as

$$\mathbf{D} = \boldsymbol{\varepsilon}\mathbf{E} \tag{5}$$

$$\mathbf{B} = \boldsymbol{\mu}\mathbf{H} \tag{6}$$

where $\boldsymbol{\varepsilon}$ and $\boldsymbol{\mu}$ are arbitrarily defined permittivity and permeability tensors. This means that the material concerned can be arbitrary, including lossless, lossy, anisotropic and dispersive media.

By utilizing the field transformation method to deal with oblique incidence, two new vectors are defined as

$$\mathbf{E}' = \mathbf{E} \cdot \exp[-j(k_x x + k_y y)] \tag{7}$$

$$\mathbf{H}' = \mathbf{H} \cdot \exp[-j(k_x x + k_y y)] \tag{8}$$

where k_x and k_y are the components of wavenumber in the x and y directions respectively, and are calculated as

$$k_x = k \cdot \sin\theta \cdot \cos\varphi \tag{9}$$

$$k_y = k \cdot \sin\theta \cdot \sin\varphi \tag{10}$$

where k is the wavenumber of the excited plane wave in free space, and θ and φ are the propagating direction angles.

Hence, the periodic boundary conditions for $\mathbf{E}'$ and $\mathbf{H}'$ are

$$\mathbf{E}'(x, y) = \mathbf{E}'(x + mT_x, y + nT_y) \tag{11}$$

$$\mathbf{H}'(x, y) = \mathbf{H}'(x + mT_x, y + nT_y) \tag{12}$$

where m and n are any integers.

In the ADE method, $\mathbf{D}, \mathbf{E}, \mathbf{B}$ and $\mathbf{H}$ are successively calculated by (1), (5), (2) and (6) respectively, where (1), (2) are material independent, and (5), (6) can be solved simply according the forms of $\boldsymbol{\varepsilon}$ and $\boldsymbol{\mu}$. Nonetheless, if only $\mathbf{E}$ and $\mathbf{H}$ are replaced by $\mathbf{E}'$ and $\mathbf{H}'$ into these four equations, the term $\exp[-j(k_x x + k_y y)]$ will appear only on one side, which will bring great difficulty in discretizing them. Therefore, another two variables are necessary to be introduced

$$\mathbf{D}' = \mathbf{D} \cdot \exp[-j(k_x x + k_y y)] \tag{13}$$

$$\mathbf{B}' = \mathbf{B} \cdot \exp[-j(k_x x + k_y y)]. \tag{14}$$

Substituting (7), (8), (13) and (14) into (5) and (6), it is obvious that no extra terms are introduced and the relations remain as

$$\mathbf{D}' = \boldsymbol{\varepsilon}\mathbf{E}' \tag{15}$$

$$\mathbf{B}' = \boldsymbol{\mu}\mathbf{H}'. \tag{16}$$

Considering the dual relation between electric and magnetic fields, (4), (7), (8), (13), and (14) are substituted only into (1), and the equations of the three components of $\mathbf{D}'$ are obtained as

$$\begin{aligned} j\omega D_x' = {} & \frac{j\omega\varepsilon_0}{j\omega\varepsilon_0 + \sigma_y}\frac{\partial}{\partial y}H_z' - \frac{j\omega\varepsilon_0}{j\omega\varepsilon_0 + \sigma_z}\frac{\partial}{\partial z}H_y' \\ & + \frac{j\omega\varepsilon_0}{j\omega\varepsilon_0 + \sigma_y} \cdot jk_y \cdot H_z' - \frac{j\omega\varepsilon_0}{j\omega\varepsilon_0 + \sigma_z} \cdot jk_z \cdot H_y' \end{aligned} \tag{17}$$

$$\begin{aligned} j\omega D_y' = {} & \frac{j\omega\varepsilon_0}{j\omega\varepsilon_0 + \sigma_z}\frac{\partial}{\partial z}H_x' - \frac{j\omega\varepsilon_0}{j\omega\varepsilon_0 + \sigma_x}\frac{\partial}{\partial x}H_z' \\ & + \frac{j\omega\varepsilon_0}{j\omega\varepsilon_0 + \sigma_z} \cdot jk_z \cdot H_x' - \frac{j\omega\varepsilon_0}{j\omega\varepsilon_0 + \sigma_x} \cdot jk_x \cdot H_z' \end{aligned} \tag{18}$$

$$\begin{aligned} j\omega D_z' = {} & \frac{j\omega\varepsilon_0}{j\omega\varepsilon_0 + \sigma_x}\frac{\partial}{\partial x}H_y' - \frac{j\omega\varepsilon_0}{j\omega\varepsilon_0 + \sigma_y}\frac{\partial}{\partial y}H_x' \\ & + \frac{j\omega\varepsilon_0}{j\omega\varepsilon_0 + \sigma_x} \cdot jk_x \cdot H_y' - \frac{j\omega\varepsilon_0}{j\omega\varepsilon_0 + \sigma_y} \cdot jk_y \cdot H_x' \end{aligned} \tag{19}$$

where k_z is zero but is kept to maintain the symmetry of each component. Considering that k_z, σ_x and σ_y are zero, and to re-

tain the uniformity and symmetry of the formulas, (17)–(19) can be rewritten as

$$j\omega D'_x = \frac{j\omega\varepsilon_0}{j\omega\varepsilon_0+\sigma_y}\frac{\partial}{\partial y}H'_z - \frac{j\omega\varepsilon_0}{j\omega\varepsilon_0+\sigma_z}\frac{\partial}{\partial z}H'_y + jk_y\cdot H'_z - jk_z\cdot H'_y \tag{20}$$

$$j\omega D'_y = \frac{j\omega\varepsilon_0}{j\omega\varepsilon_0+\sigma_z}\frac{\partial}{\partial z}H'_x - \frac{j\omega\varepsilon_0}{j\omega\varepsilon_0+\sigma_x}\frac{\partial}{\partial z}H'_x + jk_z\cdot H'_x - jk_x\cdot H'_z \tag{21}$$

$$j\omega D'_z = \frac{j\omega\varepsilon_0}{j\omega\varepsilon_0+\sigma_x}\frac{\partial}{\partial x}H'_y - \frac{j\omega\varepsilon_0}{j\omega\varepsilon_0+\sigma_y}\frac{\partial}{\partial y}H'_x + jk_x\cdot H'_y - jk_y\cdot H'_x. \tag{22}$$

To conserve space, only (22) is to be discretized in detail.

Similar to the ADE method, but without introducing extra variables f_{zx} and f_{zy}, and the corresponding precalculation [12], here D_z is directly "split" into three parts. The "split" formula is

$$D'_z = D'_{zx} - D'_{zy} + D'_{zb} \tag{23}$$

with

$$D'_{zx} = \frac{1}{j\omega+\sigma_x/\varepsilon_0}\frac{\partial}{\partial x}H'_y \tag{24}$$

$$D'_{zy} = \frac{1}{j\omega+\sigma_y/\varepsilon_0}\frac{\partial}{\partial y}H'_x \tag{25}$$

$$D'_{zb} = \overline{k_x}\cdot H'_y - \overline{k_y}\cdot H'_x \tag{26}$$

where $\overline{k_x} = \sin\theta\cdot\cos\varphi/c, \overline{k_y} = \sin\theta\cdot\sin\varphi/c$, and c is the speed of light in free space. Equation (26) is obtained by substituting (9) and (10) into the last two terms in the right side of (22).

The discrete form of (23)–(26) is

$$D'^{n+1}_{z_{i,j,k+\frac{1}{2}}} = D'^{n+1}_{zx_{i,j,k+\frac{1}{2}}} - D'^{n+1}_{zy_{i,j,k+\frac{1}{2}}} + D'^{n+1}_{zb_{i,j,k+\frac{1}{2}}} \tag{27}$$

$$D'^{n+1}_{zx_{i,j,k+\frac{1}{2}}} = \frac{1-\frac{\Delta t}{2}\cdot\frac{\sigma_x}{\varepsilon_0}}{1+\frac{\Delta t}{2}\cdot\frac{\sigma_x}{\varepsilon_0}}\cdot D'^{n}_{zx_{i,j,k+\frac{1}{2}}} + \frac{\frac{\Delta t}{\Delta x}}{1+\frac{\Delta t}{2}\cdot\frac{\sigma_x}{\varepsilon_0}}\cdot\left(H'^{n+\frac{1}{2}}_{yi+\frac{1}{2},j,k+\frac{1}{2}} - H'^{n+\frac{1}{2}}_{yi-\frac{1}{2},j,k+\frac{1}{2}}\right) \tag{28}$$

$$D'^{n+1}_{zy_{i,j,k+\frac{1}{2}}} = \frac{1-\frac{\Delta t}{2}\cdot\frac{\sigma_y}{\varepsilon_0}}{1+\frac{\Delta t}{2}\cdot\frac{\sigma_y}{\varepsilon_0}}\cdot D'^{n}_{zy_{i,j,k+\frac{1}{2}}} + \frac{\frac{\Delta t}{\Delta y}}{1+\frac{\Delta t}{2}\cdot\frac{\sigma_y}{\varepsilon_0}}\cdot\left(H'^{n+\frac{1}{2}}_{x_{i,j+\frac{1}{2},k+\frac{1}{2}}} - H'^{n+\frac{1}{2}}_{x_{i,j-\frac{1}{2},k+\frac{1}{2}}}\right) \tag{29}$$

$$D'^{n+1}_{zb_{i,j,k+\frac{1}{2}}} = -D'^{n}_{zb_{i,j,k+\frac{1}{2}}} + \overline{k_x}\cdot\left(H'^{n+\frac{1}{2}}_{y_{i+\frac{1}{2},j,k+\frac{1}{2}}} + H'^{n+\frac{1}{2}}_{y_{i-\frac{1}{2},j,k+\frac{1}{2}}}\right) - \overline{k_y}\cdot\left(H'^{n+\frac{1}{2}}_{x_{i,j+\frac{1}{2},k+\frac{1}{2}}} + H'^{n+\frac{1}{2}}_{x_{i,j-\frac{1}{2},k+\frac{1}{2}}}\right). \tag{30}$$

Based on the symmetry of electric and magnetic fields, and the cyclic features of the x, y and z components, the expressions of the other five components of $\mathbf{D}'$ and $\mathbf{B}'$ can be obtained following the same procedure. Further, through the constitutive relation, the electromagnetic fields $\mathbf{E}'$ and $\mathbf{H}'$ can be calculated conveniently.

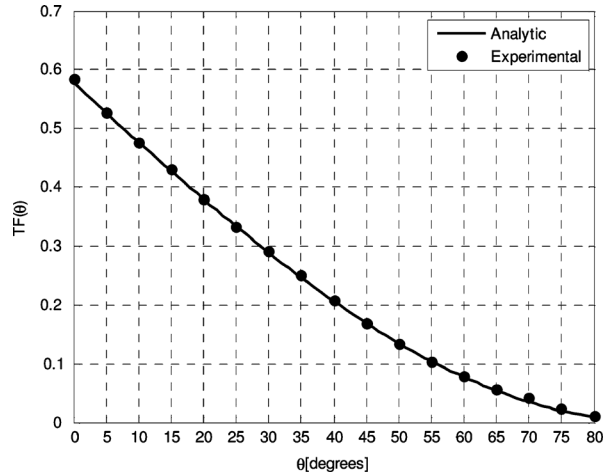

Fig. 1. Time step factor $\mathrm{TF}(\theta)$ as determined from analysis and experimental data.

It should be noted that outside the PML region, $\sigma_\eta(\eta = x, y, z)$ is zero and D'_z is reduced to the standard Yee's FDTD formulation, except for the extra term D'_{zb}. As aforementioned, the formulas of (28) and (29) can be simplified, since σ_x and σ_y in 2-D periodical structure cases are zero. Here they are presented to retain the uniformity and symmetry of all components of $\mathbf{D}'$ and $\mathbf{B}'$.

Compared to the conventional FDTD algorithm with ADE treatment, the proposed method only introduces six auxiliary parameters such as D'_{zb} and their corresponding updating operations. Therefore, the computational complexity of this method is still $O(N)$, which follows the conventional FDTD algorithm, where N is the number of Yee-cells. As the updating formulas and procedures in the calculation and PML regions are the same as those of the ADE method, it can be fully unified and integrated in an implementation in a simple manner.

B. Stability Analysis

Similar to split-FDTD [7], in the proposed method, the allowed maximum time step Δt declines as the incident angle θ increases. A simple estimate of the stability can be made from the maximum velocity in the grid, so that the expected stability of the FTM method can be given by [5] as

$$c\cdot\Delta t/\Delta s \le \mathrm{TF}\ (\theta) \tag{31}$$

where $\mathrm{TF}(\theta)$ is the time step factor $(1-\sin\theta)/\sqrt{D}$, and D is the dimensionality of the problem, 3 in this case. Although such a criterion was obtained by considering the material to be a simple medium in analysis, we observed experimentally that (31) was sufficient for the type of materials presented in this paper. As can be verified in Fig. 1, the solid line is the analytic $\mathrm{TF}(\theta)$, while the dots are found experimentally through FDTD simulation by considering general materials including dispersive media. The uniformity in Fig. 1 implies that the proposed method follows the basic criterion of the light speed limitation upon Yee grid updating.

Let us mention that in PML regions, similar to the work presented in [14], extra care need be taken to ensure the stability of the method proposed in this work. In practice, when a large

incident angle is encountered, the time step has to be small to be valid, resulting in longer simulation time. Nonetheless, the periodic unit structure involved in the simulation is in general electrically small, so that the computational time is usually acceptable. In the following examples, the choices of time step at different angles are provided, and are verified to be effective and sufficient. On the other hand, in the case of large incident angles, other methods such as those of [10] and [11] are more practical, although the re-derivation of equations needs to be implemented in terms of different media, which might be more complicated.

C. Adding the Exciting Source

In the normal incidence case, the modulated Gaussian pulse is usually adopted as the exciting source, and it is given as

$$E_i(t) = -\sin[2\pi f_0(t-t_0)]\exp\left[-\frac{2(t-t_0)^2}{\tau^2}\right] \tag{32}$$

where f_0 is the central frequency concerned, t_0 and τ control the form of the pulse and its Fourier transform $E_i(f)$. Further, in the oblique incidence case, the spectrum function is transformed as

$$E_i^{\mathrm{ob}}(f) = E_i(f)\cdot\exp[j(k_x x + k_y y)]. \tag{33}$$

Substituting (33) into (7), we obtain

$$E_i'^{\mathrm{ob}}(f) = E_i(f). \tag{34}$$

Therefore, the form of the exciting source for periodic structures at oblique incidence is the same as that of the normal case.

III. Numerical Examples

In this section, two numerical examples are implemented to demonstrate the performance of the proposed method. The first example is a Jerusalem Cross FSS (JCFSS) between two anisotropic and lossy media, as shown in Fig. 2. The response coefficients of the FSS illuminated by oblique incident plane waves at 20° and 45° are respectively calculated by the method. The second example is a photonic periodic structure with rectangular hole at a sub-wavelength scale for visible and infrared light, as shown in Fig. 6. By utilizing the dispersive Drude model, the response coefficients of the structure illuminated by a 30° oblique incident plane wave is calculated over a wideband. The numerical results of the two examples are compared with those obtained from CST for verification. In addition, the increments of memory usage in the two examples are both no more than 10%, compared to the simulation using a conventional FDTD program in the normal incidence case. Therefore, it can be seen that a significant increase of computational complexity is not introduced to the FDTD algorithm in the proposed method.

A. Jerusalem Cross FSS With Anisotropic and Lossy Media

The JCFSS stuck in the middle of two anisotropic and lossy media is shown in Fig. 2. The unit cell period is 6 mm, the thickness of the medium is 2 mm, and the thickness of the JCFSS is 0.625 mm. The model is simulated by using the proposed method with space intervals $\Delta x = \Delta y = \Delta z = 0.125$ mm,

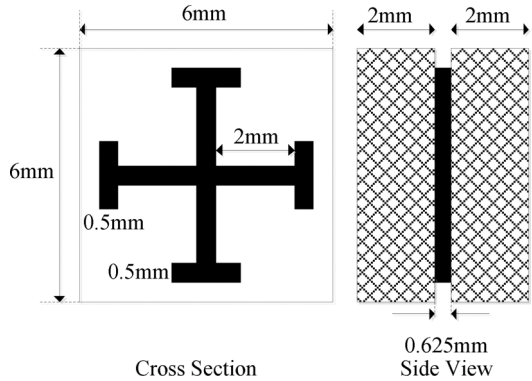

Fig. 2. Schematic diagram of the JCFSS.

excited by an oblique incident TM mode ($\theta = 20°, \Delta t = \Delta x/(10\cdot c)$) and a TE mode ($\theta = 45°, \Delta t = \Delta x/(20\cdot c)$) respectively. The transmission and reflection coefficients are calculated over a wideband from 5 GHz to 25 GHz. The relative permittivity and conductivity tensors of the medium are given as

$$\boldsymbol{\varepsilon_r} = \begin{bmatrix} 2.2 & 0 & 0 \\ 0 & 1.1 & 0 \\ 0 & 0 & 1.5 \end{bmatrix} \quad \boldsymbol{\sigma} = \begin{bmatrix} 0.05 & 0 & 0 \\ 0 & 0.03 & 0 \\ 0 & 0 & 0.01 \end{bmatrix}. \tag{35}$$

The transient pulses of the incident, transmitted and reflected electric fields in the case of $\theta = 20°$ are presented in Fig. 3, and the reflection coefficients for the two angles are shown in Figs. 4 and 5. From the comparison, it can be seen that good agreement is obtained between the results of the proposed method and those of CST. From the difference between the solid and dotted curves in Figs. 4 and 5, the feature of the anisotropic medium is clearly shown. It is worthwhile to point out that, the wideband frequency response of the FDTD method is obtained by fast Fourier transformation of the pulses recorded in the time domain through a single transient calculation, as shown in Fig. 3, and any expected sampling interval in the frequency domain can be obtained through zero-padding in the time domain before Fourier transformation. Moreover, the memory usage of the FDTD simulation is 59 MB on a computer with an Intel Core, 2.53 GHz processor, which is approximately 10% more than that of the same model simulated by the conventional FDTD program at normal incidence.

B. Photonic Periodic Structure With Rectangular Hole at a Sub-Wavelength Scale

The extraordinary transmission through periodic arrays of sub-wavelength holes [15] has been intensively studied in recent years. The widely accepted explanation is that the surface plasmon, which is supported by metals, such as silver or gold, is the fundamental condition for the extraordinary transmission. The Drude model [16] is frequently used to calculate the electromagnetic field through structures formed of dispersive metals, and the permittivity is expressed as

$$\varepsilon(\omega) = \varepsilon_0\left(\varepsilon_r - \frac{\omega_p^2}{\omega^2 - j\omega v}\right). \tag{36}$$

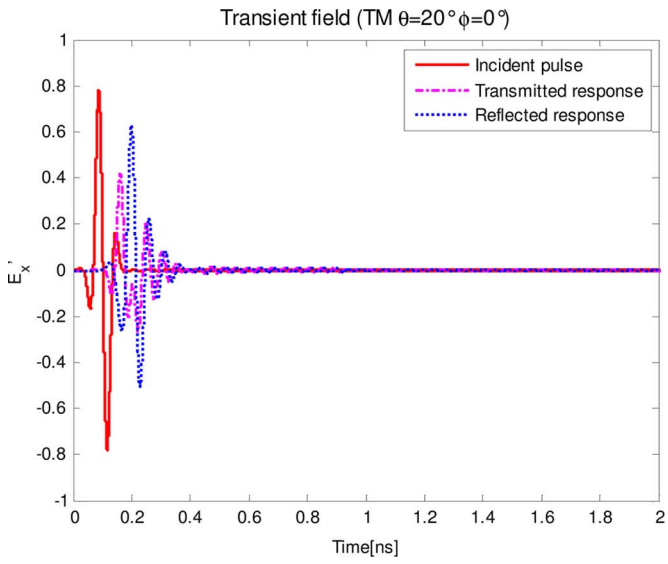

(a)

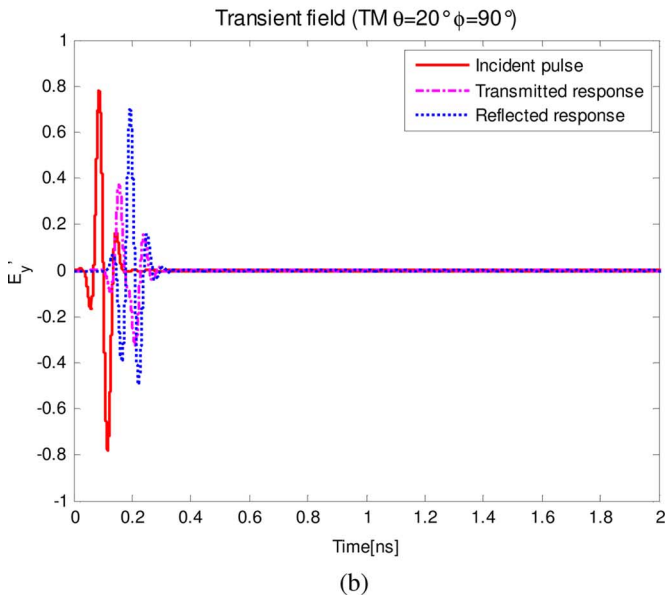

(b)

Fig. 3. Transient electric fields for the JCFSS in the case of TM mode of oblique incident ($\theta = 20°$); (a) $\varphi = 0°$; (b) $\varphi = 90°$.

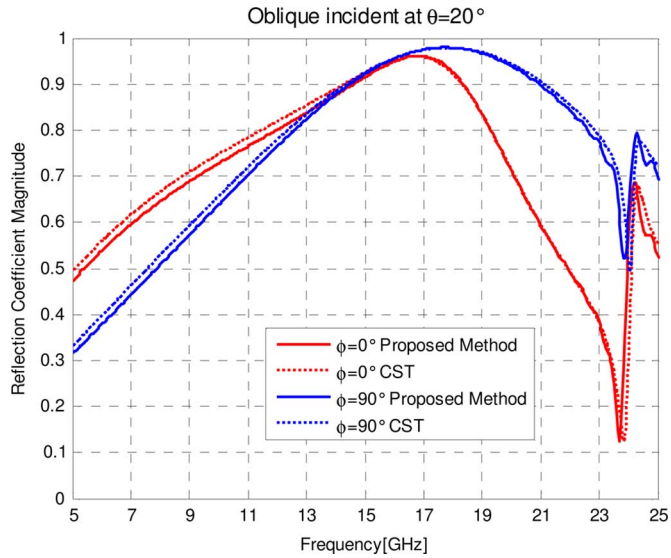

Fig. 4. Reflection coefficients for the JCFSS in the case of TM mode of oblique incident ($\theta = 20°$).

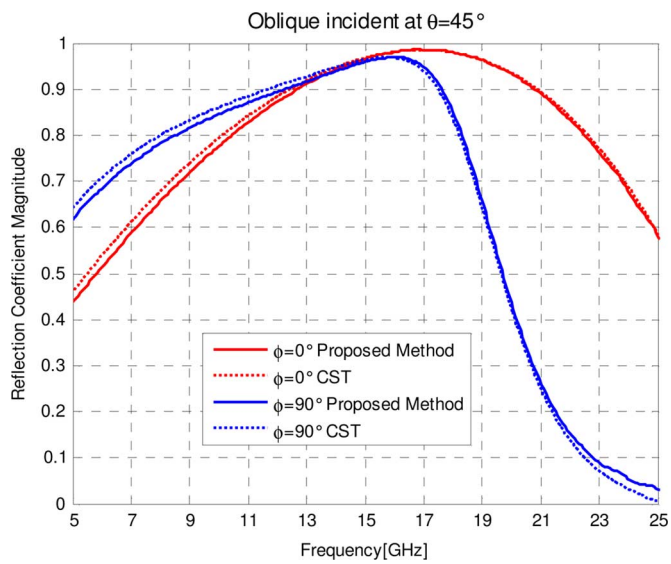

Fig. 5. Reflection coefficients for the JCFSS in the case of TE mode of oblique incident ($\theta = 45°$).

In this example, the unit cell of a photonic periodic structure with a rectangular hole at a sub-wavelength scale, as shown in Fig. 6, is calculated in the range of wavelength from 450 to 1000 nanometers. The variables in (36) are given as: $\varepsilon_r = 8.3$, $\omega_p = 1.672 \times 10^{16}$ rad/s and $\nu = 3 \times 10^{13}$ Hz. The exciting plane wave is the TE mode at $\theta = 30°$ and $\varphi = 50°$, and the reflection and transmission coefficients are calculated by the proposed method with space intervals $\Delta x = \Delta y = \Delta z = 2.5$ nm ($\Delta t = \Delta x/(15 \cdot c)$). CST results are also given.

The transmission and reflection coefficients are shown in Fig. 7. It can be seen that, the solid and dotted lines are almost identical, including the area of resonance, which successfully demonstrates the validity of this method in dealing with second-order dispersive media. In the FDTD simulation, it takes 194 MB of memory usage using the same computer as the first example, and it is approximately 9% more than that of the same model simulated by the conventional FDTD program at normal incidence.

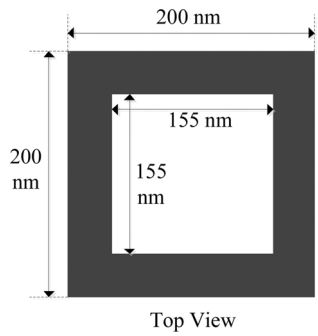

Fig. 6. Schematic diagram of the unit cell of a photonic periodic structure of silver, with rectangular hole, the thickness is 105 nm.

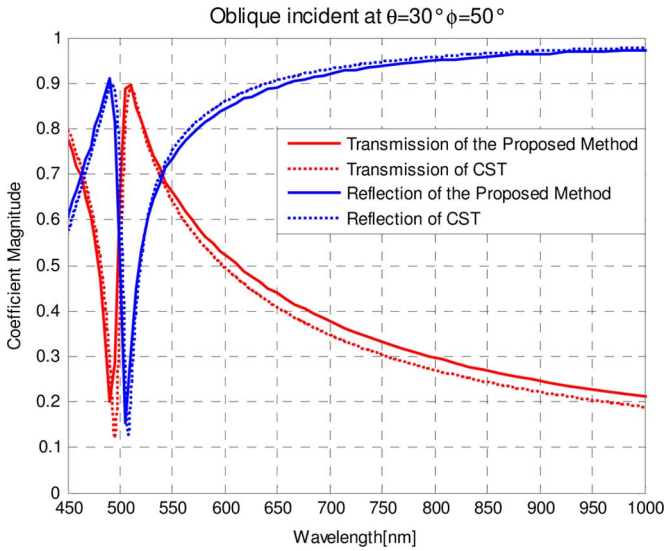

Fig. 7. Transmission and Reflection coefficients for the periodic arrays of sub-wavelength holes in the case of TE mode of oblique incident ($\theta = 30°, \varphi = 50°$).

IV. Conclusion

This paper introduces a novel wideband FDTD approach to analyze periodic structures excited by oblique incident plane waves. The approach is based on the field transformation method to remove the time gradient, and splits each component of the transformed fields of the electric displacement vector and the magnetic induction intensity vector into three parts in a simple manner. The proposed method can be fully integrated with ADE PML update formulation and procedures, leading to a much simpler implementation. Unlike previous methods that generally deal with a specific type of simple medium, this method is unified in form and is material independent. A first example in the millimeter wave band with an anisotropic lossy medium and a second in the light region with a dispersive medium are respectively calculated over wide bands. The results show good agreement with those of CST, which well validates the proposed method.

References

[1] B. A. Munk, *Frequency Selective Surfaces: Theory and Design*. New York, NY, USA: Wiley, 2000.

[2] T. Wu, *Frequency Selective Surface and Grid Array*. New York, NY, USA: Wiley, 1995.

[3] R. Mittra, C. H. Chan, and T. Cwik, "Techniques for analyzing frequency selective surfaces—A review," *Proc. IEEE*, vol. 76, no. 12, pp. 1593–1615, Dec. 1988.

[4] N. Amitay, V. Galindo, and C. P. Wu, *Theory and Analysis of Phased Array Antennas*. New York, NY, USA: Wiley, 1972.

[5] A. Taflove and S. C. Hagness, *Computational Electrodynamics*. Norwood, MA, USA: Artech House, 2000.

[6] P. Harms, R. Mittra, and W. Ko, "Implementation of the periodic boundary condition in the finite-difference time-domain algorithm for FSS structures," *IEEE Trans. Antennas Propag.*, vol. 42, no. 9, pp. 1317–1324, Sep. 1994.

[7] J. A. Roden *et al.*, "Time-domain analysis of periodic structures at oblique incidence: Orthogonal and nonorthogonal FDTD implementations," *IEEE Trans. Microw. Theory Tech.*, vol. 46, no. 4, pp. 420–427, Apr. 1998.

[8] J.-B. Wang, B. Chen, and B.-H. Zhou, "Improved split-field method for solving oblique incident wave on periodic structures," *Electron. Lett.*, vol. 47, no. 16, pp. 898–900, 2011.

[9] J. Wang *et al.*, "Unconditionally stable FDTD method for solving oblique incident plane wave on periodic structures," *IEEE Microw. Wireless Compon. Lett.*, vol. 21, no. 12, pp. 637–639, Dec. 2011.

[10] Z.-Y. Cai *et al.*, "The WLP-FDTD method for periodic structures with oblique incident wave," *IEEE Trans. Antennas Propag.*, vol. 59, no. 10, pp. 3780–3785, Oct. 2011.

[11] J. Wang *et al.*, "Weakly conditionally stable FDTD method for analysis of 3D periodic structures at oblique incidence," *Electron. Lett.*, vol. 48, no. 7, pp. 369–371, 2012.

[12] O. Ramadan, "Auxiliary differential equation formulation: An efficient implementation of the perfectly matched layer," *IEEE Microw. Wireless Compon. Lett.*, vol. 13, no. 2, pp. 69–71, Feb. 2003.

[13] Q. Liu, "An FDTD algorithm with perfectly matched layers for conductive media," *Microw. Opt. Technol. Lett.*, vol. 14, no. 2, pp. 134–137, Feb. 1997.

[14] S. Abarbanel, D. Gottlieb, and J. S. Hesthaven, "Long time behavior of the perfectly matched layer equations in computational electromagnetics," *J. Scientif. Comput.*, vol. 17, no. 1–4, pp. 405–422, 2002.

[15] K. K. Koerkamp *et al.*, "Strong influence of hole shape on extraordinary transmission through periodic arrays of subwavelength holes," *Phys. Rev. Lett.*, vol. 92, no. 18, p. 183901, 2004.

[16] N. Garcia and M. Bai, "Theory of transmission of light by sub-wavelength cylindrical holes in metallic films," *Opt. Exp.*, vol. 14, pp. 10028–10042, 2006.

Bin Liang received the B.Sc. degrees in electronic and information engineering from the Beihang University, Beijing, China, in 2008, and is currently pursuing the Ph.D. degree at the same university.

Since 2008, he has been a Research Assistant at Beihang University. His research interests include frequency selective surfaces, electromagnetic band-gap structures, and computational electromagnetic.

Ming Bai received the B.Sc. and Ph.D. degrees in physics, from the University of Science and Technology of China (USTC), Hefei, Anhui, China, in 1996 and 2002, respectively.

From 2002 to 2006, he was a Postdoctoral Researcher with the Laboratory of Nanotechnology (LFSP), Spanish National Research Council (CSIC). Since 2006, he has been an Associate Professor with the School of Electronic and Information Engineering, Beihang University, Beijing, China. His current research interests include microwave imaging and computational electromagnetics.

Hui Ma received the B.Sc. degrees in electronic and information engineering from the Beihang University, Beijing, China, in 2009, and is currently pursuing the Ph.D. degree at the same university.

Since 2009, she has been a Research Assistant at Beihang University. Her research interests include antennas, microwave imaging, and passive surface-space bi-static SAR.

Naiming Ou received the B.Sc. degree in electronic and information engineering and the Ph.D. degree in electromagnetic and microwave technology from the Beihang University, Beijing, China, in 2008 and 2013, respectively.

Since 2008, he has been a Research Assistant with the Microwave Engineering Laboratory, Beihang University. His current research interests include computational electromagnetics, compact antenna test range, and microwave imaging techniques.

Jungang Miao received the B.S.E.E. degree from the National University of Defence Technology, Changsha, China, in 1982, the M.S.E.E. degree from the Beihang University, Beijing, China, in 1987, and the Dr. Rer. Nat. degree in physics from the University of Bremen, Bremen, Germany, in 1998.

From 1982 to 1984, he was with the Institute of Remote Sensing Instrumentation, Chinese Aerospace, Beijing, China, where he developed space-borne microwave remote sensing instruments. From 1984 to 1993, he was with the Electromagnetic Laboratory, Beihang University, doing research and teaching in the field of microwave remote sensing. In 1993, he joined the Institute of Environmental Physics and Remote Sensing, University of Bremen, Bremen, Germany, as a staff member conducting research on space-borne microwave radiometry. In October 2003, he returned to Beihang University, and since then, he has been the Chair Professor with the Electromagnetic Laboratory. His research areas are electromagnetic theory, microwave engineering, and microwave remote sensing of the atmosphere, including sensor development, calibration, and data analyses.